ELSEVIER

Polymer 40 (1999) 2089–2102

polymer

On deformation mechanisms of β-polypropylene 2. Changes of lamellar structure caused by tensile load

J.X. Li[a,*], W.L. Cheung[b], C.M. Chan[a]

[a]*Department of Chemical Engineering, Advanced Engineering Materials Facility Hong Kong University of Science and Technology, Clear Water Bay, Hong Kong*

[b]*Department of Mechanical Engineering, The University of Hong Kong, Pokfulam Road, Hong Kong*

Received 10 March 1998; revised 18 May 1998; accepted 18 May 1998

Abstract

Several β-polypropylene (β-PP) samples were stretched to various strains at room temperature. The morphologies of the deformed specimens were studied by scanning electron microscopy and transmission electron microscopy. The deformation was highly inhomogeneous in the β-PP specimens. In the early stage of deformation, horizontal lamellae were stretched to separation and deformation bands were formed within a spherulite in some regions. The deformation bands coalesced as strain increased. Near the yield point, some deformation bands developed into crazes across the spherulite boundaries. Meanwhile, melting spots and shear bands were found in the yielded sample. However, the main cause of failure was cracking across the specimen.

Keywords: β-Polypropylene; Deformation mechanisms; Morphology

1. Introduction

In the past 40 years, many aspects of plastic deformation of crystalline plastics, including morphological changes during deformation, have been studied extensively. Most of the theoretical and experimental studies have been concentrated on linear polyethylene (PE). Several models associating the plastic deformation with the structure changes of PE crystals can be found in the literature [1,2]. Prior to Peterlin's model [3] (lamella breaking and reorganization) and Flory's hypothesis [4] (crystal melting and recrystallization), Peterson [5] first put forward that the plastic deformation of crystalline plastics was related to the movement of screw dislocations in lamellae. Actually, Peterson's suggestion is an extension of the conventional theory of crystal plasticity. Owing to the long chain feature of polymers, however, such dislocation movement should be of {*hk*0} [00*c*] chain slip systems [6], i.e. the slip planes should contain the chain axes.

Following Peterson's work, Young and coworkers [7,8] measured the variation of the critical resolved shear stress (CRSS) for {010} [001] chain slip in a single-crystal texture high density (HD) PE as a function of temperature. Their measured values of CRSS fitted the theoretical curve for crystals 5 nm thick, whereas the average thickness of the lamellae as indicated by SAXS was 20 nm. This was interpreted as a result of the variation of the thickness both among lamellae and within an individual lamella. Dislocations would be generated in the thinnest sites where it is most energetically favorable.

The structure changes in lamellae caused by stretching at room temperature were directly examined using a transmission electron microscope (TEM) by Thomas and coworkers on a single-crystal-like HDPE film [9]. They found that at low strain the deformation was accommodated entirely in the interlamella regions and for strain beyond 300% stretching-induced crystallization occurred in the extended amorphous regions. On further deformation, two chain slip systems, {100} [001] and {010} [001], were clearly visualized. The observed chain slip could be resolved into small continuous chain slip (fine slip) and large block shear (coarse slip). On even higher strain, breaking up of lamellae through intralamella shear took place. It was believed [10,11] that the sheared blocks would ''decrystallize'' when their dimensions became less than a critical size and contributed to the formation of long crystalline microfibrils. The ''decrystallization'' might operate via chain slip, crystal shear and defect generation within the interior of the mosaic blocks of PE lamellae.

* Corresponding author.

0032-3861/99/$ - see front matter
PII: S0032-3861(98)00412-1

Bartczak and coworkers investigated the changes in texture of spherical and textured HDPE during compression deformation [12,13]. Based on their analysis of WAXS pole figures and a sudden inverse variation of SAXS long period, combined with the observation of morphologies, they concluded that in the initial stage of compression deformation, the amorphous layers whose normals were perpendicular to the loading direction would extend in the flow direction while other amorphous layers would shear and rotate. Further deformation would cause slip in the lamellae. Consequently, the lamellae were stretched out and became thinner. The continually thinning lamellae became unstable and periodic pinching-off might occur when the lamellae were thin enough [13]. Once the lamellae were pinched off, the fragments could change their shape to reduce potential energy and touch to form new lamellae perpendicular to the flow direction by migration of the accumulated defects.

Now, it is normally accepted that in much of the irreversible plastic deformation of textured PE and thin PE film, the mechanisms involved are mostly crystallographic in nature, especially crystallographic slip in the chain direction; meanwhile, some deformation mechanisms acting in the amorphous layers between lamellae are also involved in the early stage of the deformation process. The simultaneous activity of several deformation mechanisms allows the initial PE structure to be transformed into the final orientated state. Owing to the complexity of spherulites, the deformation mechanisms in bulk-crystallized plastics under applied stresses are, perhaps, more complex.

In a series of studies on deformation mechanisms of β-polypropylene (β-PP), previous WAXS and differential scanning calorimeter (DSC) experiments [14] have demonstrated that when β-PP samples were stretched at room temperature, the β-phase transformed to α-phase after necking. Based on the difference between the spatial distribution of the molecular chains in the β-phase and α-phase crystals, it has been concluded that the β-phase PP crystals were stretched to melting locally during cold drawing and the melting might initiate from some of the defects in the crystals. In this study, compression-molded β-PP samples, which consisted of mostly β-phase spherulites before deformation, were stretched to various strains. The deformation mechanisms of β-PP related to the lamellar structural changes of the β spherulites caused by a tensile load were investigated using a scanning electron microscope (SEM) and a TEM. Several deformation mechanisms for the strains up to yielding were identified.

2. Experiment

2.1. Sample preparation

For preparation of the β-PP sample, a doped PP resin, containing 0.6% of β-nucleating agent [15,16], was placed in a stainless steel mold and melted in a hot press at 200°C for 5 min; then it was quickly moved to another press and molded into a 2.0 mm thick slab. The sample was allowed to crystallize isothermally at 130°C for 25 min under pressure. After isothermal crystallization, the slab was removed from the press and cooled to room temperature naturally. The slab was milled into dumb-bell-shaped specimens. Their dimensions were about 11 mm wide and 80 mm long. The overall crystallinity of the prepared sample and the percentage of the β phase were determined, using a DSC, to be 62% and 84% respectively.

2.2. Tensile deformation

The tensile specimens were stretched uniaxially on a Lloyd LR 50K tensile testing machine with a cross-head speed of 5.0 mm min^{-1} at room temperature. The specimens elongated more or less uniformly within the whole gage length and showed stress-whitening after yielding. No obvious cold drawing occurred on the specimens during testing until the specimens broke at a strain of approximately 120%. The crystallinity of the α and β phases of the deformed samples was measured using a DSC and the results are summarized in Table 1. The percentage of the β phase was generally unaffected by the tensile load even after yielding; however, it was reduced for the broken specimen.

The strain of the deformed specimens before yielding was recoverable at room temperature. The permanent strain for the specimen stretched to a strain of 5.0% (yielding point) was about 0.5% after relaxation for 1 week. As the strain was increased to 10% and 100%, the permanent strain was 1% and 24% respectively after relaxation. In order to determine the relationship between the structural changes and the yielding process, the specimens that were subjected

Table 1
The percentage of β phase of deformed β-PP at various strains

Strain (%)	β-melting point (°C)	α-melting point (°C)	ΔH_β (J g^{-1})	ΔH_α (J g^{-1})	X_β (%)	X_α (%)	ϕ_β (%)
0	155.5	167.0	87	19	51	11	83
5	155.5	167.0	90	16	53	9	85
70	156.0	167.5	89	18	52	10	84
115	155.7	167.1	80	27	47	15	75

X_i: crystallinity of a crystalline phase.
ϕ_β: percentage of β phase.

to loading levels of 50%, 90%, and 100% of the yield load were selected for morphology investigation in detail. The corresponding strains of the specimens, determined from the elongation of the gage length under load, were 1.5%, 3.6%, and 5.0% respectively.

2.3. Permanganic etching

The deformed specimens were first allowed to relax for more than 6 months at room temperature. They were then trimmed on the flank along the loading direction with a Leitz 1400 microtome until one-third of the specimen width was removed. The microtomed surface was further trimmed with a Reichert Ultracut E microtome equipped with a glass knife to produce an extremely smooth surface for permanganic etching [17].

The etchant was composed of 0.5 wt% potassium permanganate in a mixture of concentrated sulfuric acid and phosphoric acid in a 3:2 volumetric ratio. The trimmed specimen was immersed in the etchant at about -5°C. The beaker containing the etchant was placed in an ultrasonic bath. After etching for 20 min, the specimens were washed in chilly 30 wt% sulfuric acid, then in 30% hydrogen peroxide, distilled water and acetone. Finally, they were dried in a desiccator.

2.4. SEM examination

The samples were coated with gold–platinum using a Bio-Rad SEM coating system operating at 1.2 kV and 15 mA. A multi-step coating process was adopted in order to avoid possible damage to the fine structure of the etched sample due to overheating. A coating period of 30 s was chosen in each run and a total of eight runs were employed. SEM examination was performed on a Cambridge S360 scanning electron microscope and the investigation was made in the central position of the etched surface.

2.5. RuO_4 staining

The deformed specimens were cut into thin strips perpendicular to the loading direction. The cross-section of the strips was about $0.2 \times 0.3\ mm^2$. They were embedded in an epoxy resin and cured at 40°C for 48 h. The embedded specimens were first trimmed with a razor blade and then with an ultracut microtome equipped with a glass knife. An extremely smooth trapezoidal top surface was obtained with the cross-section of the polymer strip. For staining, the trimmed specimens were exposed to vapor of ruthenium tetroxide [18] in a sealed test tube for a period of 24 h at room temperature. After staining, the specimens were washed in a 3 wt% aqueous solution of sodium periodate and distilled water, and then finally dried in a desiccator.

2.6. Ultramicrotomy and TEM examination

A Reichert Ultractut E microtome was used for ultrathin microtomy. The top layer (about 1 μm) was first removed from the stained specimen using a glass knife (45°); then, ultrathin sections of about 50 nm thick were cut with a Diatome diamond knife (35°) at room temperature. The cutting speed was $1.5\ mm\ s^{-1}$ for the glass knife and

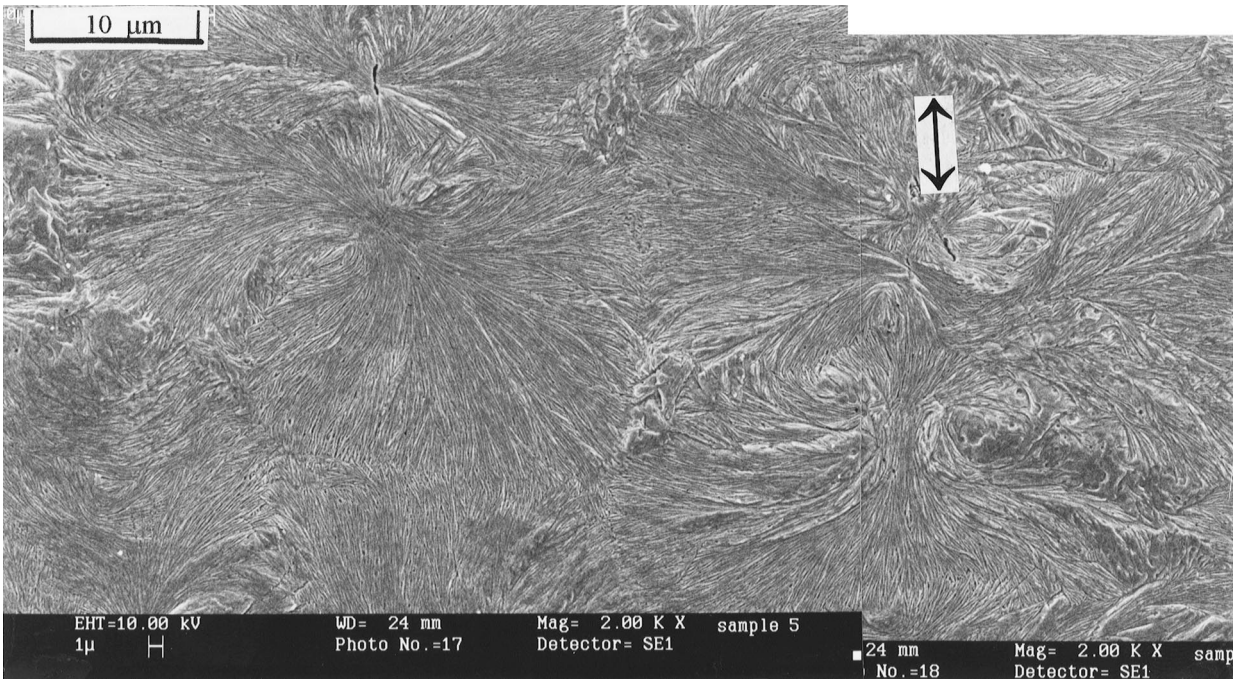

Fig. 1. SEM micrograph of β-PP sample stretched to 1.5% with 50% of yield load, showing an overall view of lamellar structure. The arrow indicates the loading direction.

1.0 mm s^{-1} for the diamond knife. The ultrathin sections were mounted on 200 mesh copper grids and dried in a desiccator. Finally, they were examined using a Jeol JEM-100SX TEM operating at an accelerating voltage of 80 kV.

3. Results and discussion

3.1. Morphology at 1.5% strain

Fig. 1 shows an SEM micrograph of a sample subjected to a strain of 1.5%. As on undeformed samples [19], the spherulites (sheaf-like lamellae) can easily be identified on the deformed specimen. The spherulites have a random orientation and some of them have an asymmetrical appearance due to limited space for growth. No obvious structural changes are observed compared with the undeformed specimen. At a higher magnification, as shown in Fig. 2, however, fine slits could be found in certain regions where the lamellae were perpendicular to the loading direction. These slits run along the lamellae and most of them were about 1 μm long, but a few could be up to several micrometers (as marked with A and B in Fig. 2). The slits occurred within the spherulites and seldom passed across the spherulite boundaries.

The slits should be the deformation bands and contain the deformed material before etching. Although the strain was only 1.5% and was recoverable after unloading, the actual strain might be highly inhomogeneous in the specimen and the local strain could be considerably larger in some interlamella layers between the horizontal lamellae (the stretching direction is vertical) due to the lower modulus of the amorphous material. The molecules in these interlamella layers might be highly extended along the loading direction, thus inducing destruction of the original structures of the contiguous lamellae. During etching, the highly deformed material was removed along with the amorphous material, leaving slits on the surface of the etched specimens.

The results observed are very different from the conclusions deduced from the study on polymer films. For polymer films, the spherulite boundaries are believed to contain more amorphous material and should deform more easily. Indeed, the spherulite boundary in polymer films may be weaker than other regions of the spherulites because of the smaller thickness, resulting from the volume contraction on crystallization. In a sample bulk-crystallized under pressure, however, the relative variation of thickness in the specimens should be small and the spherulite boundary is no longer the weakest portion; therefore, the deformation does not occur in the spherulite boundaries only. In fact, a TEM examination [19] indicated that the spherulite boundaries of the β-PP sample do not contain any more amorphous phase than other regions of the spherulites. The morphology of the boundaries between the β spherulites depends on the contact angles between the lamellae of the neighboring spherulites. If two sets of lamellae of two adjacent spherulites are growing in opposite directions then no clear boundary can be identified between them.

3.2. Morphology at 3.6% strain

On the specimen stretched to 3.6% at a stress level of 90% of the yielding stress, more slits along lamellae were

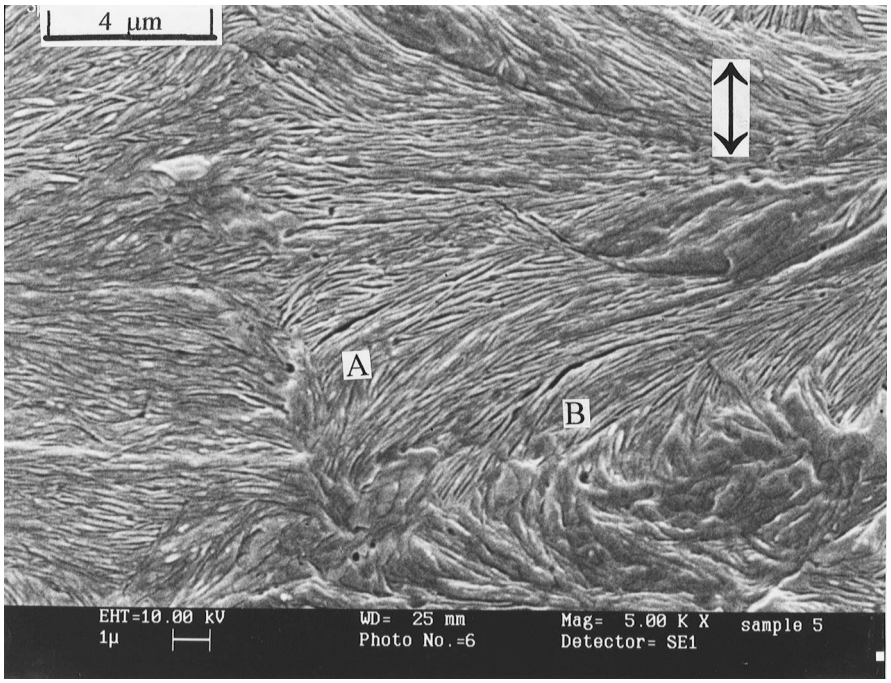

Fig. 2. SEM micrograph of β-PP at 1.5% strain under closed examination. (A) and (B): slits running along lamellae within spherulites. The arrow indicates the loading direction.

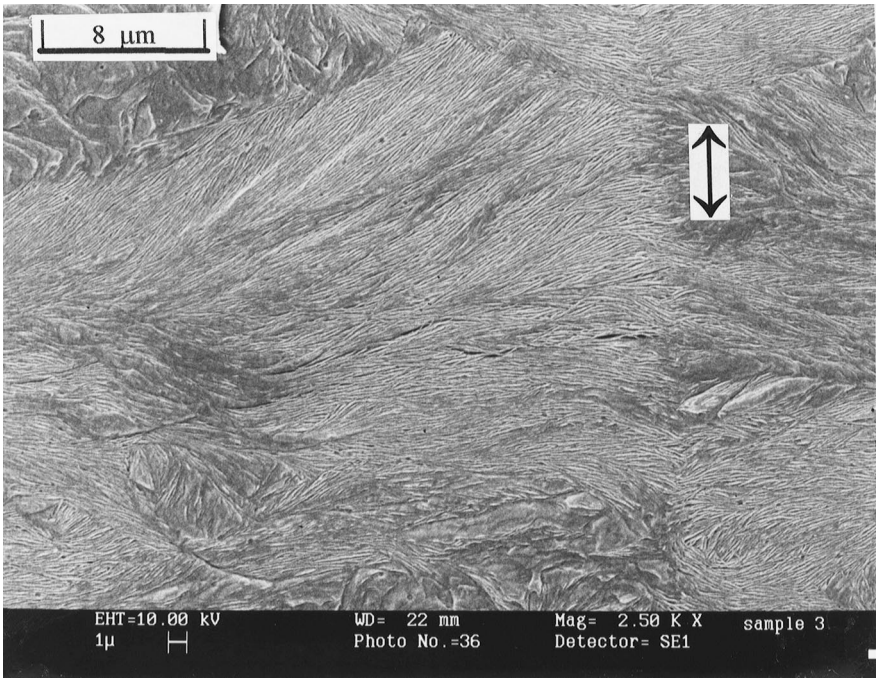

Fig. 3. SEM micrograph of β-PP sample at 3.6% strain, showing connection of fine slits. The arrow indicates the loading direction.

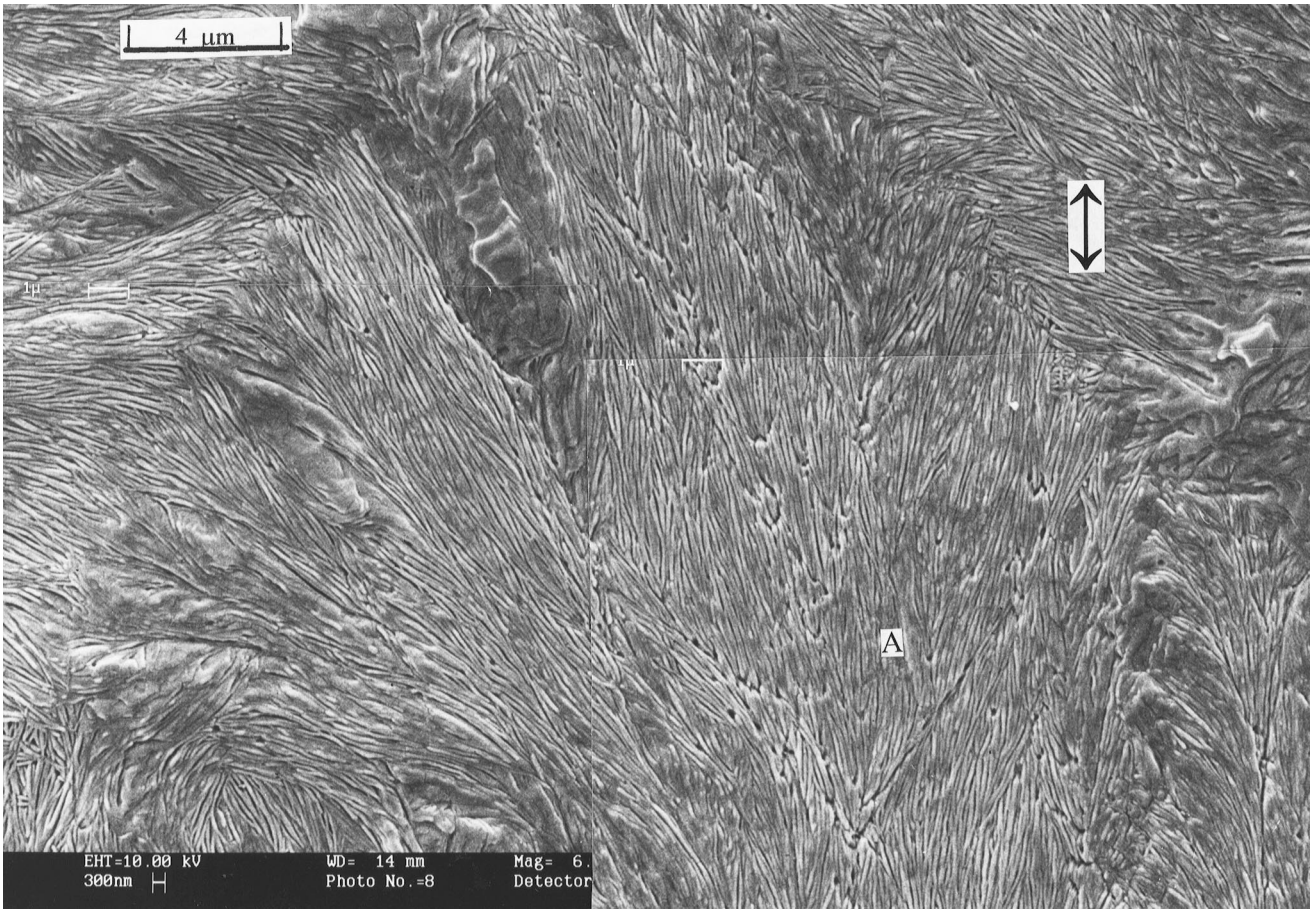

Fig. 4. SEM micrograph of β-PP sample at 3.6% strain. In area A the lamellae are roughly along the loading direction and were stretched to breaking. The arrow indicates the loading direction.

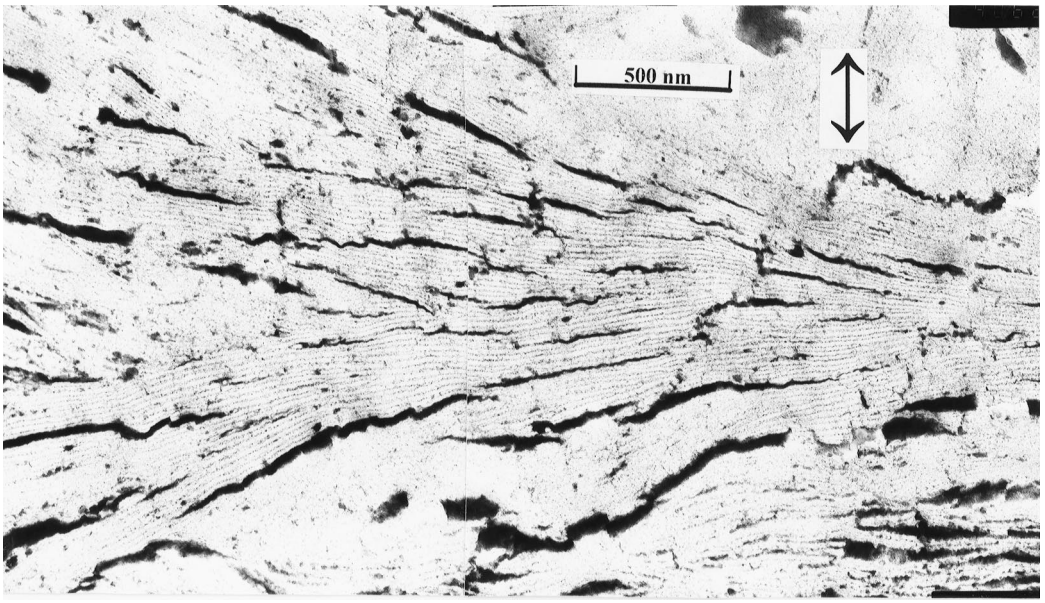

Fig. 5. TEM micrograph of β-PP sample at 3.6% strain, showing deformation bands along lamellae. The arrow indicates the loading direction.

observed in the horizontal lamella regions (the loading direction is vertical), as shown in Fig. 3. Some slits coalesce and connect to form bigger ones. However, the slits are still within the spherulites and the majority of them are about 3 μm long; occasionally, slits longer than 10 μm could be found. At this strain, apart from the slits along the horizontal lamellae, some vertical lamellae were found to have been stretched to breaking. Fig. 4 is another SEM micrograph of the sample at 3.6% strain. In the region marked A the lamellae are roughly along the loading direction. It can be seen that many of the lamellae appear to be broken. In contrast, in the adjacent region, where the lamellae have a predominately horizontal orientation, many fine slits along the lamellae are observed.

Fig. 5 is a TEM micrograph of the β-PP sample at 3.6% strain. The arrow on the TEM micrograph indicates the loading direction. From Fig. 5 one can see that some dark bands are present between lamellae within a spherulite. These dark bands are about 40 nm wide and several hundred nanometers long. They are more or less perpendicular to the loading direction. It is believed that the dark bands in the TEM micrographs and the fine slits observed in the SEM micrographs should reflect the same structure (deformation bands along lamellae) because the damaged lamellae

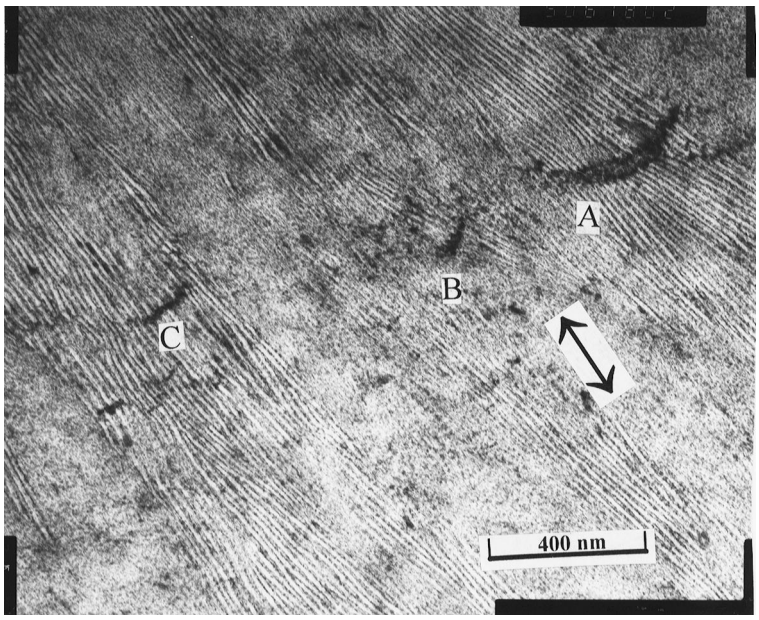

Fig. 6. TEM micrograph of β-PP sample at 3.6% strain. (A), (B) and (C): local disintegration of lamella bands which are along the loading direction. The arrow indicates the loading direction.

absorbed RuO_4 during staining and, consequently, appear as dark bands in the TEM micrographs. During etching the damaged lamellae were removed by the etchant, leaving fine slits on the etched surface.

Fig. 6 is another TEM micrograph showing the lamellae orientating along the loading direction. It can be seen that some lamella bundles were broken and a few dark stripes (marked with A, B and C) were formed running approximately perpendicular to the loading direction. The dark stripes appear to be similar to the slits running across vertical lamellae (Fig. 4). The dark stripes are not open cracks but the deformed material which has absorbed a higher content of ruthenium tetroxide. The lamellae at these areas have been transformed into a disordered state under a tensile load, i.e. some vertical lamellae were stretched to disintegrate locally.

The above SEM and TEM results clearly show that at a stress level of 90% of the yield stress the horizontal lamella (lamellae perpendicular to the loading direction) might be stretched to separation, leading to the formation of deformation bands, whereas the vertical lamellae could be stretched to breaking locally. Evidently, in the horizontal lamella region there was more amorphous material capable of extension in the loading direction, whereas the vertical lamellae took more load due to a higher modulus; thereby, the local stress concentration might induce local distortions or even the disintegration of the vertical lamellae.

3.3. Morphology at 5% strain

When the strain increased to about 5%, the specimen began to yield. On the yielded specimen the observed structure changes are similar to those observed on the specimen at a strain of 3.6%, but, as the material was stretched more, the structure changes became greater and were more striking, especially for the slits along lamellae. Fig. 7 is an SEM micrograph of the β-PP sample just after yielding. It can be seen that the coarse slits run along lamellae across almost

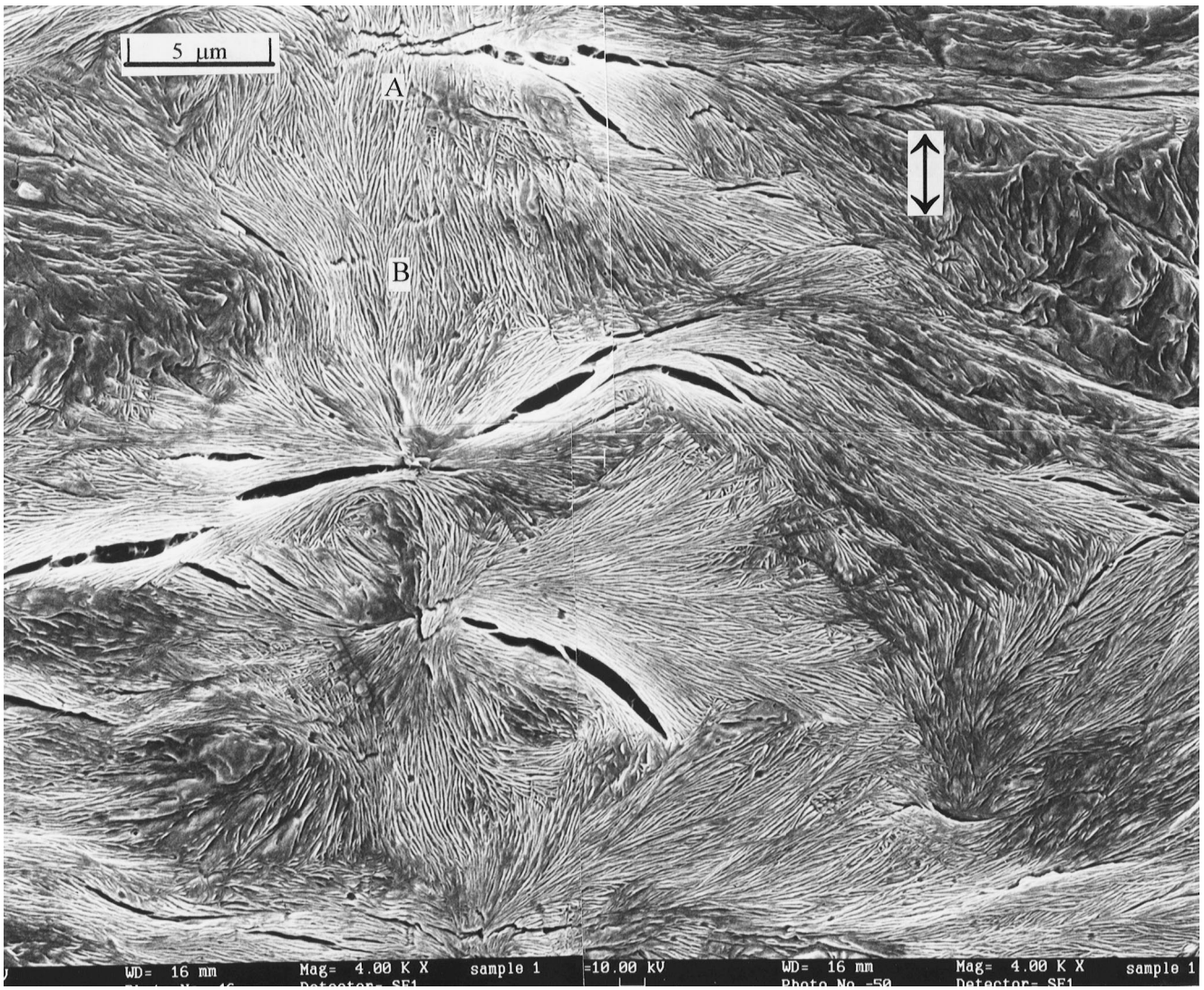

Fig. 7. SEM micrograph of β-PP at yield point, crazing along horizontal lamellae across almost whole spherulite and occasionally across the vertical lamellae (A). (B): broken lamella band. The arrow indicates the loading direction.

the whole horizontally oriented spherulite (in the middle of the micrograph). Also, two adjacent slits can cut across vertical lamellae between them and connected together (marked A on the top of the micrograph). Furthermore, when the specimen was stretched to yielding, the slits were no longer confined within individual spherulites and some of them crossed the spherulite boundaries to coalesce with slits in neighboring spherulites, as shown in Fig. 8. The slits in the yielded β-PP are up to 1 μm wide and tens of micrometers long. Perhaps, some of the coarse slits are crazes or cracks before etching. Actually, after the specimen was stretched to its yielding point, further straining resulted in the emergence of long slits across several spherulites and finally the formation of cracks across the specimen. This is consistent with the observed stress-whitening after yield during testing.

Fig. 9 is a TEM micrograph of the yielded specimen and shows the development of cracks in β-PP sample under a tensile load. In this micrograph, fully developed crazes (crack) can be seen. Also, some highly deformed materials can be found bridging the two sides of some of the crazes (see the areas marked by A, B and C). Furthermore, when two crazes (D and E) were about to coalesce, the intervening material (including lamellae) became highly distorted, leaving a dark band on the RuO_4 stained sections. Crazing is a common phenomenon in glassy polymers under tension. The crazes appear as small crack-like entities and are oriented perpendicular to the tensile axis. In classical crazes, microfibrils bridge the two sides of the craze, taking the applied stress. However, the ''crazes'' observed in the yielded β-PP sample are different from the classical crazes observed in glassy polymers. They are bridged by distorted materials instead of highly drawn microfibrils.

Fig. 10 shows the morphology near the end of a crack. A few fine dark shuttle-like articles (marked by A) could be found among the lamellae. The dark shuttles look wider and

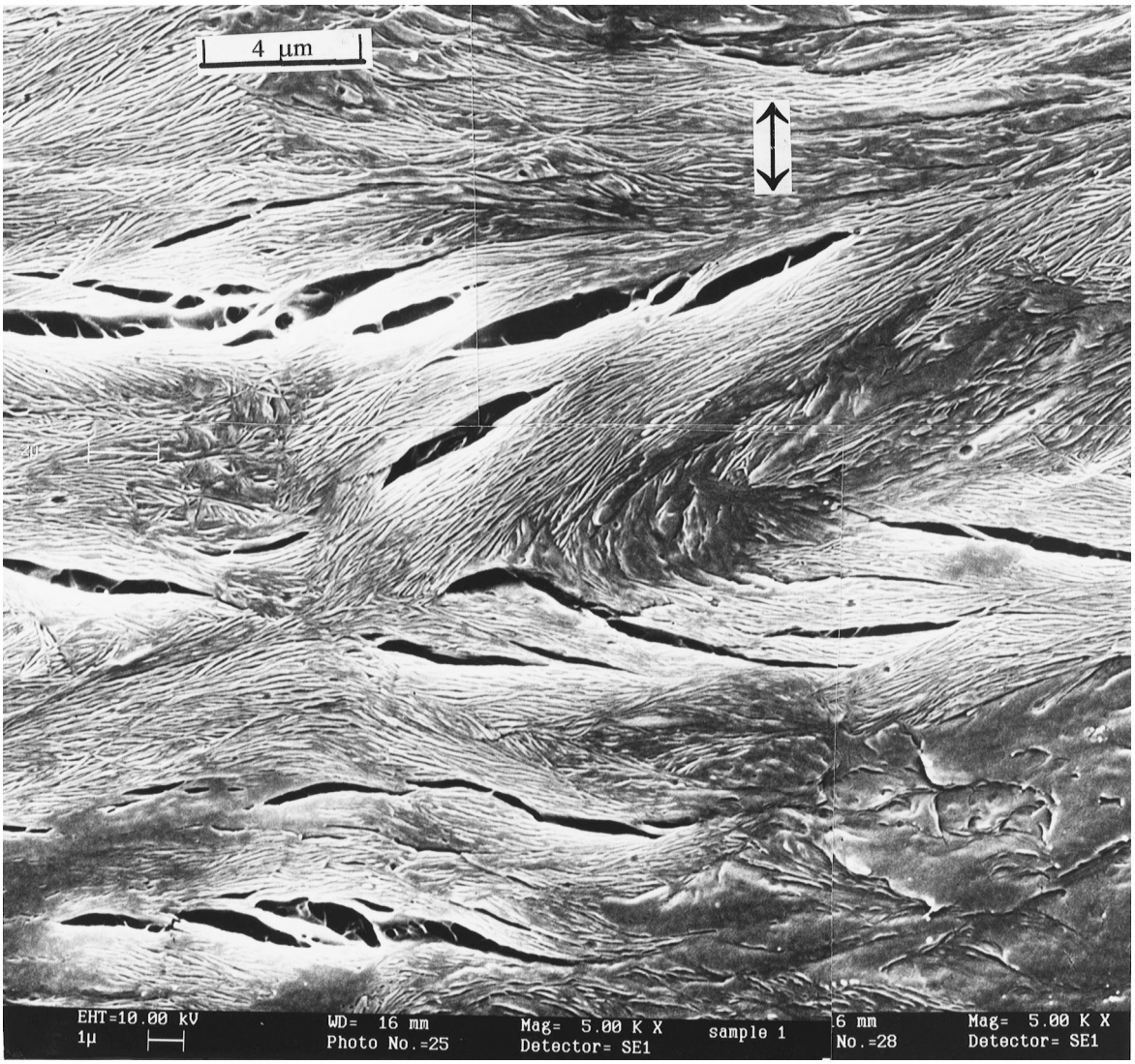

Fig. 8. SEM micrograph of yielded β-PP at 5.0% strain, showing coalescence of crazes across neighboring spherulites. The arrow indicates the loading direction.

darker than the adjacent amorphous layers. Next to the dark shuttles, the lamellae appear to be narrower and even became dark. Similar dark shuttle-like articles were also found in Fig. 9 (marked by F, G and H); however, the size of those shuttle-like articles appears larger. The big one is about 50 nm wide and 400 nm long and looks more like a deformation band. It is believed that the dark shuttle-like article in Fig. 10 is the embryo for a deformation band resulted from the separation of lamellae. Under a tensile load, the interlamella layers perpendicular to the loading direction would extend more in the stress direction, resulting in lamellae separation. This causes the distortion and destruction of the ordered structure of the contiguous lamellae and initiates the formation of deformation bands. Continual interlamella separation would lead to the growth of deformation bands and the formation of crazes and cracks.

Fig. 11 shows another TEM micrograph of the sample at 5% strain. Although the stretching direction is parallel with the lamellae, some areas show extensive shear deformation perpendicular to the lamellae. There is a distinctive shear band near the top right-hand corner of the micrograph (marked A). The thickness of the shear band is about 200 nm and the shear displacement between the upper and lower sides of the band is about 200 nm. Despite the amount of shear displacement, the lamellae in the shear band remain unbroken but become tilted at a large angle to the original orientation of the lamellae. The lamellae in the sheared section are much thinner than the unsheared parts and some appear rather vague, indicating that the lamellae were about to disintegrate. The shear band is an obvious example of intralamella slip as proposed by Bowden and Young [1]. It occurred most likely due to shear stress parallel with the chain axis in the lamellae and such shear stress could be generated as a result of an inhomogeneous deformation within the material. In comparison, another shear band near the bottom right corner (see area B) shows little sign of major reduction in the lamella thickness. The development of such shear bands primarily involved the shear deformation in the amorphous layers between the lamellae, i.e. interlamella shear.

Apart from the shear bands, some round spots can be observed in the TEM micrograph (areas marked C and D in Fig. 11). In these areas the amount of shear deformation is relatively insignificant. The morphology within these spots is very different from the surrounding β lamellae. Fig. 12 shows such a spot which exhibits a structure somewhat similar to the cross-hatched structure of an α-PP spherulite. The bright strips within the spots are believed to be lamellar

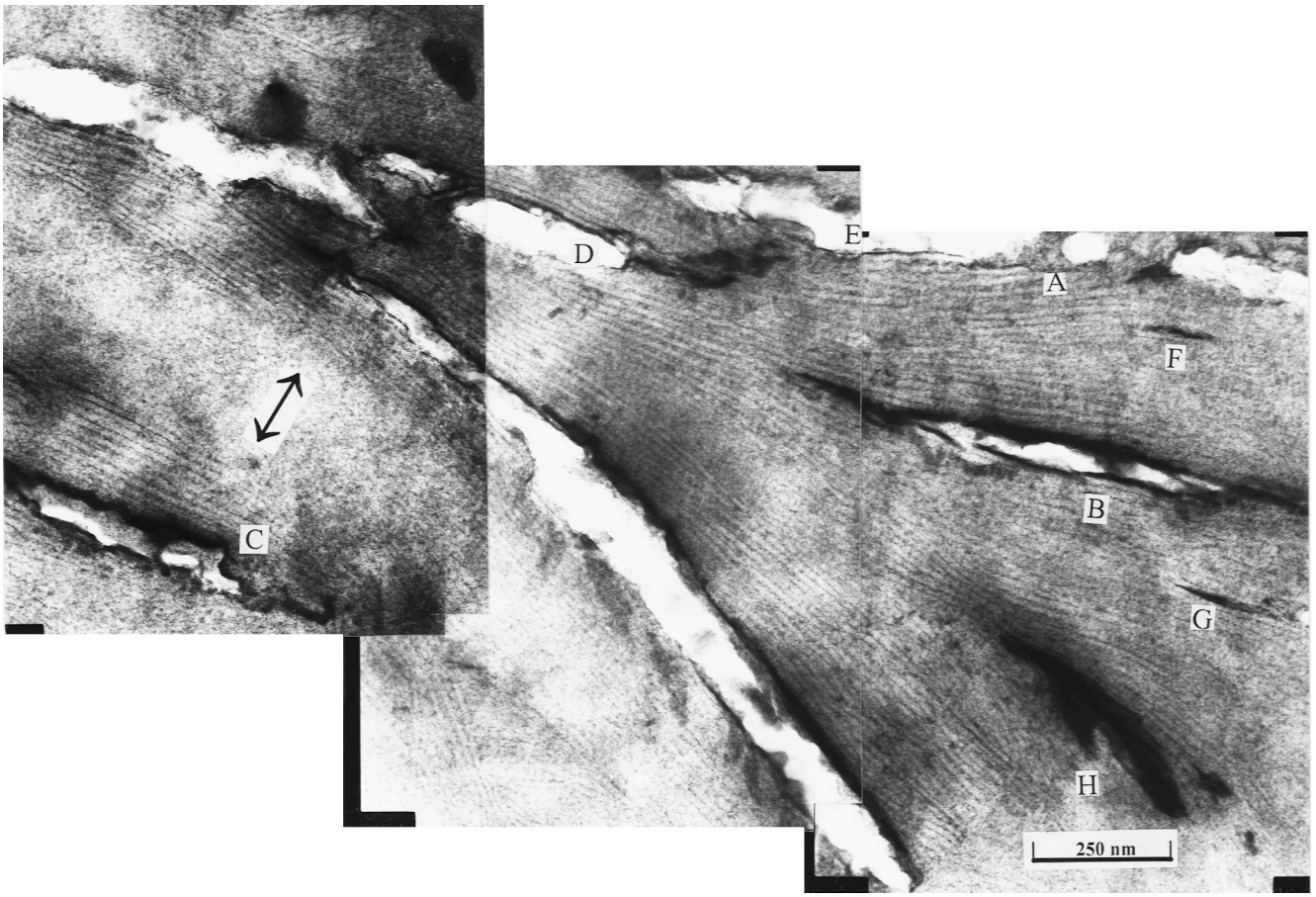

Fig. 9. TEM micrograph of yielded β-PP at 5.0% strain. (A), (B), (C), (D) and (E): crazes developed along lamellae; (F), (G) and (H): deformation bands. The arrow indicates the loading direction.

crystals, but they are much finer than the surrounding β lamellae. In some spots the fine lamellar structure appears to have a preferred orientation and the surrounding β lamellae also appear to have been sheared in the same direction, as shown in Fig. 13. From the arrangement of the β lamellae around the spot, it is obvious that the β lamellae were connected before generation of the spot. The formation of the spots is probably associated with the β-α phase transformation, i.e. as the ''melting'' of the β-phase crystals followed by recrystallization of the melt [14].

The above melted spots seem to be contrary to the DSC results of the deformed specimens (see Table 1). As shown in Table 1, the DSC results indicate that the percentage of the β-phase did not change after yielding. However, it should be pointed out that the deformation was highly inhomogeneous in the material and the total volume of the melt spots was small compared with the whole specimen; hence, the amount of the β-α phase transformation was insignificant and the DSC could not detect such small changes. However, a reduction in the crystallinity of the β phase was detected using the DSC for the broken β-PP specimen (see column 8 in Table 1). The TEM and SEM results indicated that the coalescence of crazes caused additional disintegration of the lamellae between the crazes as the strain increased.

The melting of the lamellae is a mechanically induced process. Under a tensile load, the crystals of the sample were distorted and the internal energy of the sample should increase, especially in the areas where the lamellae are parallel with the loading direction, because in these areas the tensile strains were generally the same in both lamella and amorphous regions; thus, the vertical lamellae will take up more of the acting load. The increase in the internal energy may increase the probability that the chain segments within the crystals jump away from the equilibrium lattices. When the tensile stress increases beyond a certain level, the internal energy may be high enough to permit the lamellae to disintegrate at rather high rates, i.e. mechanically induced melting.

Using a deformation calorimeter, Rudnev et al. [20] found that less than 50% of the input mechanical work was converted into heat during the deformation of plastics and the rest was stored in the deformed material. Their experiments also showed that the stored energy in a crystalline PET sample was considerably higher than that in an amorphous PET sample, indicating that the stored energy is related more to distortion of the crystals. It is likely that certain localized areas within the material possess a large amount of stored energy. This will decrease the thermal stability of the crystals and these highly stressed lamellae may decrystallize or ''melt''. It should be pointed out that mechanically induced melting of the crystals does not necessarily occur at the normal melting temperature. In the presence of external stresses, melting is possible at lower temperature.

The glass transition temperature of PP is about -10°C. After the β lamellae were stretched to such an extent that decrystallization occurred, the material was in a rubbery state at room temperature. The large deformation might cause the alignment of some of the chain segments and reduce the conformational entropy, resulting in strain-induced crystallization, which is commonly observed in elastomeric materials [21–24]. The oriented crystals in the sheared melt spot (see Fig. 13) were probably formed under such conditions. The cross-hatched structure in some of the melt spots (see Fig. 12) might form in those areas with a relatively low strain after deformation; then, the resultant crystals are expected to be similar to those crystallized under normal conditions.

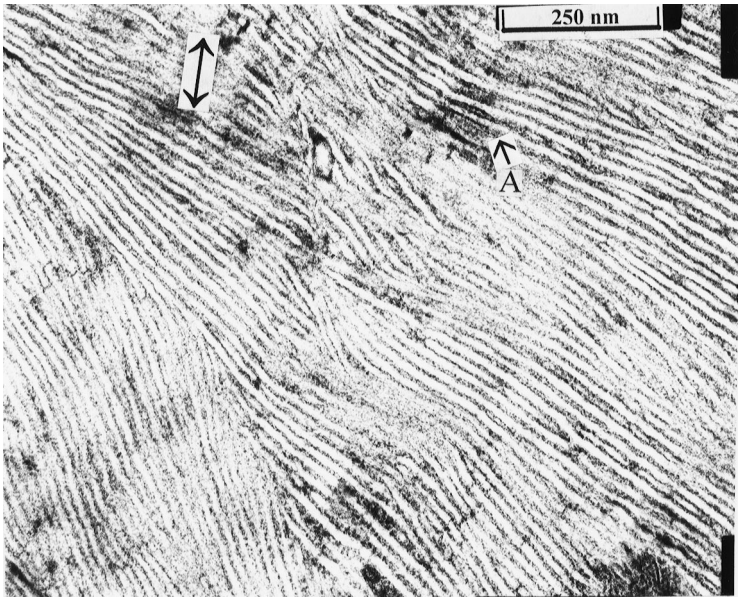

Fig. 10. TEM micrograph near the end of deformation bands in the yielded β-PP sample: (A) an embryo of deformation band. The arrow indicates the loading direction.

Fig. 14 shows another TEM micrograph of the yielded sample at 5% strain. In the melt spot near the upper left corner of the micrograph, it is surprising to find that a β-lamella survived the ''melting'' process. Nevertheless, the thickness of the lamella section within the melt spot is smaller than other sections outside the melt spot and the lamella section has an ''S'' shape, indicating that the lamella section was sheared slightly. The shear deformation and reduction of the lamella thickness are a result of fine chain slipping within lamellae, as proposed by Bowden and Young [1]. It is not fully understood why a particular lamella section can stay whole while the surrounding materials have gone through the ''melting'' process. Perhaps, the shear deformation helped to release some of the stored energy and prevented the ''melting'' of the crystals. This also explains why no melt spots are found in areas where many shear bands or deformation bands exist. On the upper right-hand side of the same

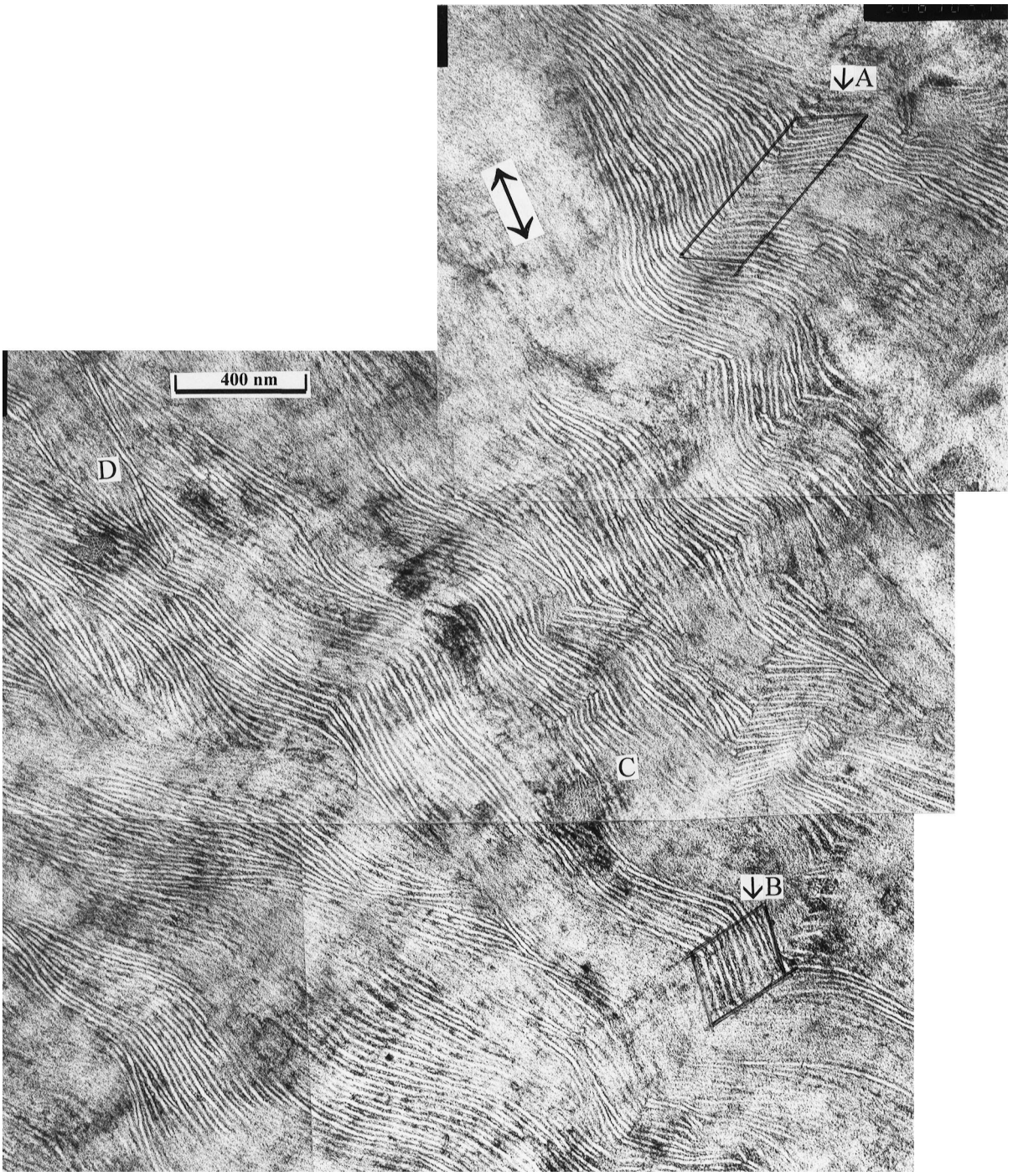

Fig. 11. TEM micrograph of yielded β-PP at 5.0% strain, (A): shear band caused by intralamella slipping and interlamella shear; (B): shear band primarily caused by interlamella shear; (C) and (D): melt spots. The arrow indicates the loading direction.

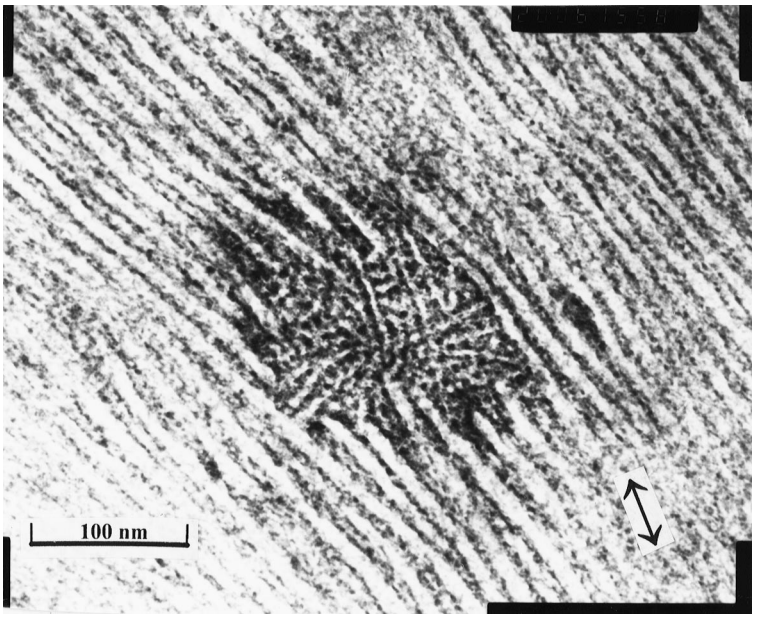

Fig. 12. TEM micrograph showing a melt spot with cross-hatched structure observed in β-PP sample at yield point. The arrow indicates the loading direction.

melt spot, a β lamella looks like a bamboo after several of its sections became thinner. Obviously, these sections were about to decrystallize. This observation is consistent with the work of Brady and Thomas [10,11] which indicated that when a lamella block is reduced to a size less than the critical size through chain slipping it would become thermodynamically unstable and decrystallize at the deformation temperature.

Occasionally, long dark bands were found in the yielded specimen, as shown in Fig. 15. They cut across lamellae approximately perpendicularly, taking a similar orientation to the crazes. They are believed to be the deformation bands marked A and B in Fig. 7. Sometimes, a few melt spots could be seen located on such bands. These bands are believed to have formed due to further deformation of the materials between the melt spots. When a melt spot is formed, the stresses in the melted material are relaxed and these stresses are transferred to the surroundings of the melt spot. Consequently, this process may cause the widening of the melt spot or the formation of new melt spots nearby. On further straining, the undeformed materials between the melt spots will be subjected to higher stresses, leading to the formation of these continuous deformation bands.

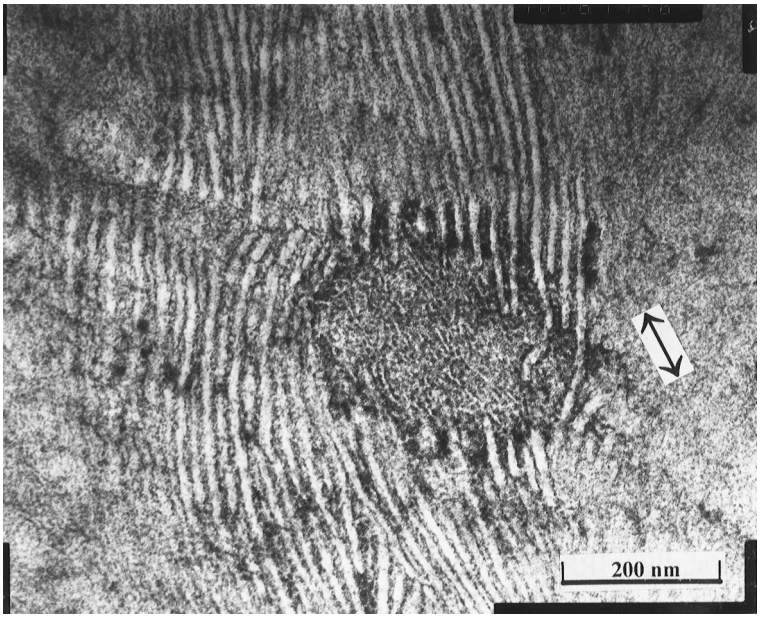

Fig. 13. A melt spot in yielded β-PP observed under TEM; lamellae in the melt spot possess a preferred orientation due to shear stress. The arrow indicates the loading direction.

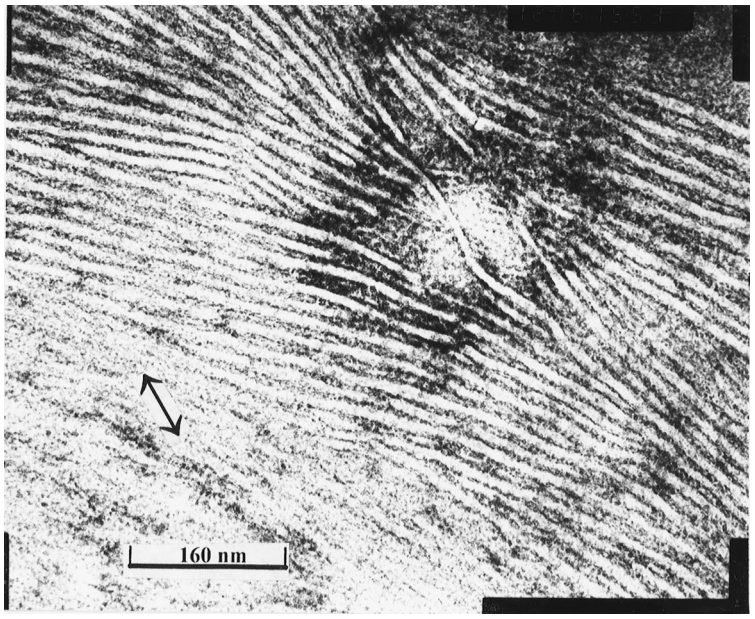

Fig. 14. TEM micrograph of yielded β-PP at 5.0% strain, the melt spot contains β-lamellae which survive the melting process. The arrow indicates the loading direction.

4. Conclusions

Separation of lamellae, which mainly occurred in the area where the lamellae were perpendicular to the loading direction, resulted in the formation of deformation bands. On further deformation, these deformation bands developed into crazes and cracks. Intralamella slipping took place mostly in the areas where the lamellae were along the loading direction. In this case, the lamellae could be stretched to distortion and disintegration, leading to the formation of melting spots. In addition, shear bands might form in the vertical lamellae through the cooperation of interlamella shear and intralamella slipping.

In the early stage of deformation, horizontal lamellae were stretched to separation, leading to the formation of deformation bands within the spherulites. The deformation bands could coalesce as strain increased. Near the yielding point, some vertical lamellae were stretched to disintegration or breaking locally. When the sample was stretched to the yielding point, some of the deformation bands could develop into crazes across the spherulite boundaries and lamellae in front of them. Melt spots and shear bands occurred in the yielded sample. However, the main cause

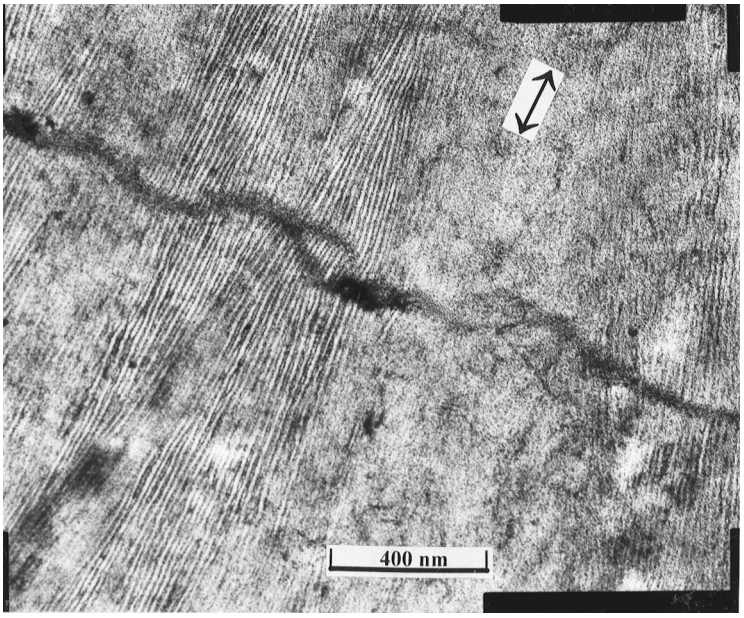

Fig. 15. Continuous deformation band across lamellae in yielded β-PP at 5.0% strain observed under TEM. The arrow indicates the loading direction.

of failure for the sample was crazing. Adjacent small crazes connected together and developed into large cracks across the spherulites. The sample was broken by the emergence of the cracks across the specimen.

Acknowledgements

The authors would like to thank the staff of the Electron Microscopy Unit of the Hong Kong University for assistance with operation of the microscopes and printing micrographs.

References

[1] Bowden PB, Young RJ. J Mater Sci 1974;9:2034.
[2] Porter SR, Wang LH. J Macromol Sci Rev Macromol Chem Phys C 1995;35(1):63.
[3] Peterlin A. J Mater Sci 1971;6:490.
[4] Flory PJ, Yoon DY. Nature 1978;272:226.
[5] Peterson JM. J Appl Phys 1966;37:4047.
[6] Shadrake LG, Guiu F. Philosophical Magazine 1976;34:565.
[7] Young RJ. Philosophical Magazine 1974;30:85.
[8] Young RJ, Bowden PB, Rider JG. J Mater Sci 1973;8:23.
[9] Adams WW, Yang D, Thomas EL. J Mater Sci 1986;21:2239.
[10] Brady JM, Thomas EL. J Mater Sci 1989;24:3311.
[11] Brady JM, Thomas EL. J Mater Sci 1989;24:3319.
[12] Bartczk Z, Cohen RE, Argon AS. Macromolecules 1992;25:4692.
[13] Bartczk Z, Galeski A, Argon AS, Cohen RE. Macromolecules 1992;25:5705.
[14] Li JX, Cheung WL. Polymer, in press.
[15] Li JX, Cheung WL. J Vinyl & Additive Tech 1997;3:151.
[16] Li JX, Cheung WL. J Mater Process Tech 1997;63:472.
[17] Norton DR, Heller A. Polymer 1985;26:704.
[18] Li JX, Ness JN, Cheung WL. J Appl Polym Sci 1996;59:1733.
[19] Li JX, Cheung WL. Polymer, submitted.
[20] Rudnev SN, Salamation OB, Voenniy VV, Oleynik EF. Colloid Polym Sci 1991;269:460.
[21] Flory PJ. Chem Phys 1947;15:3976.
[22] Treloar R. The physics of rubber elasticity, 3rd ed. Oxford: Clarendon Press, 1974.
[23] Holl B, Kiliam HG, Schenk H. Collid Polym Sci 1990;268:205.
[24] Ward IM, Hadley DW. An introduction to the mechanical properties of solid polymers. Chichester: Wiley, 1993, p. 41.